Modified Switching-Table Strategy for Reduction of Current Harmonics in Direct Torque Controlled Dual-three Phase Permanent Magnet Synchronous Machine Drives

K. D. Hoang, Y. Ren, Z.Q.Zhu*, M. Foster

***Abstract*—The switching-table-based direct torque control strategies (ST-DTC) of dual-three phase permanent magnet synchronous machine (PMSM) drives are investigated in this paper. Owing to its inherited advantage of suppression of sixth harmonic torque pulsation, dual-three phase machine has attracted more and more interests among various sorts of multi-phase machines. However, unexpected stator harmonic currents are often observed in the classical ST-DTC strategy for dual-three phase PMSM drives, which cause large losses and decrease the efficiency of the drive system. An optimized ST-DTC strategy which consists a two-step process to determinate the most appropriate inverter voltage vector is proposed to reduce the stator harmonic currents. The merits of the classical direct torque control, i.e. simple structure and good dynamic performance, are still preserved. The experimental results verify that the proposed method can significantly reduce the current harmonics.**

***Index Terms*— direct torque control (DTC), dual-three phase, harmonic stator currents, permanent magnet synchronous machines (PMSM).**

The authors are with the Department of Electronic and Electrical Engineering, University of Sheffield, Sheffield, S1 3JD, U.K. (E-mail: khoa_hoang78@yahoo.com; y.ren@sheffield.ac.uk; Z.Q.Zhu@sheffield.ac.uk, Tel: +44(0)1142225360, Fax: +44(0)1142225196; m.p.foster@sheffield.ac.uk).

Nomenclature

G_i	Voltage vector group
L_s	α and β axis inductance
L_{ls}	Stator leakage inductance
L_m	Magnetizing inductance in $\alpha\beta$ subspace
P	Number of pole pairs
R_s	Stator resistance
T_e	Electromagnetic torque
T_s	Sampling period
$\boldsymbol{V}_{s\alpha\beta}$, $\boldsymbol{\psi}_{s\alpha\beta}$, $\boldsymbol{I}_{s\alpha\beta}$	Stator voltage, flux and current vectors in $\alpha\beta$ subspace
$\boldsymbol{V}_{sz1z2}$, $\boldsymbol{\psi}_{sz1z2}$, $\boldsymbol{I}_{sz1z2}$	Stator voltage, flux and current vectors in z_1z_2 subspace
$\boldsymbol{V}_{so1o2}$, $\boldsymbol{\psi}_{so1o2}$, $\boldsymbol{I}_{so1o2}$	Stator voltage, flux and current vectors in o_1o_2 subspace
ω_1	Machine angular velocity
ε_ψ ,ε_T	Stator flux and torque control signals
θ_r	Electrical rotor position
$\theta_{s\alpha\beta}$, θ_{sz1z2}	Position of stator flux vector in $\alpha\beta$ subspace and z_1z_2 subspace
$\boldsymbol{\psi}_{r\alpha\beta}$	Rotor flux vectors in $\alpha\beta$ subspace
ψ_s, ψ_r	Amplitude of stator and rotor flux vector in $\alpha\beta$ subspace
ψ_{s_ripple}, T_{e_ripple}	Ripple of stator flux and torque

1 Introduction

Recently, the interest in multiphase machine drives has considerably increased, especially for high-power and/or high-current applications such as aerospace applications, ship propulsion, electric/hybrid vehicles, and renewable energy generation. In these applications, the controlled power can be shared by more inverter legs to reduce the current stress of each semiconductor device compared to three-phase converters [1]. Other potential advantages of the multiphase machine drives are higher reliability at the system level, lower torque pulsations, and lower dc-link voltage requirement [2, 3].

A very interesting and well-discussed type of multiphase machines is the dual-three phase machine having two sets of three-phase windings spatially shifted by 30 electrical degrees, as shown in Fig.1. In the dual-three phase machine, the sixth harmonic torque pulsation, which is predominant in the three-phase systems, will be completely absent because of the opposition of these

components produced by two sets of windings [4]. Nevertheless, large stator circulating harmonic currents will occur in the voltage-source-inverter (VSI) fed dual-three phase machine since the machine impedance associated with these harmonics is very small - only composed of the stator resistance and leakage inductance, according to the machine model using vector space decomposition approach (VSD) [5]. These unexpected harmonic currents cause extra losses and require higher semiconductor device ratings [6].

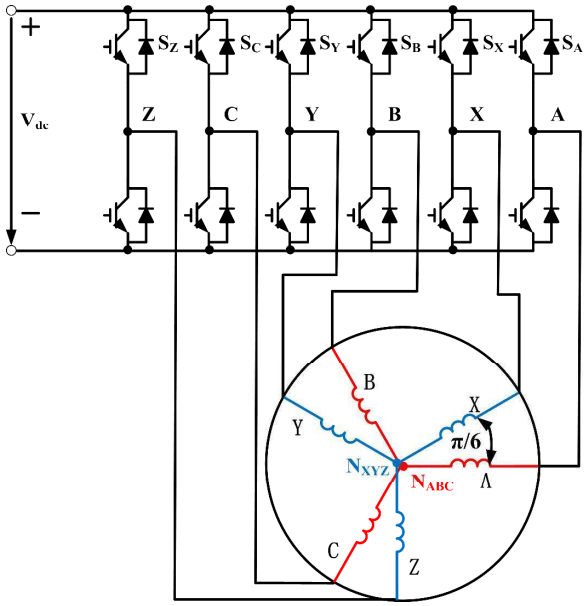

Fig. 1. *Voltage-source-inverter-fed dual-three phase PMSM and drive*

Previous investigations have been conducted to explore vector control using suitable pulse-width-modulation (PWM) techniques and to extend its theory for dual-three phase machine drives [1, 7]. Although unexpected stator harmonic currents can be minimized under these strategies, complicated and time-consuming calculation is essentially required.

On the other hand, direct torque control (DTC) strategy is an applicable alternative because of its simple structure, excellent transient response and good robustness against machine parameters. Based on the vector space decomposition technique [5], only the variables in $\alpha\beta$ subspace in the dual-three phase system relate to the torque, which is similar to the case in three phase drives. Therefore, the classical switching-table-based DTC (ST-DTC) strategy can be easily extrapolated to dual-three phase drives. However, the classical DTC strategy suffers from the aforementioned large stator harmonic currents because of lacking controlling of harmonic components in z_1z_2 subspace. Hatua etc. [8] develops two new methods of ST-DTC technique, called Resultant Flux Control Method and Individual Flux Control Method, for the dual-three phase machine drive to reduce the torque ripple, however, the unexpected stator harmonic currents still exist. Harmonic suppression schemes have been dedicated for the ST-DTC of five-phase machines [9-11].

This paper aims to reduce the stator harmonic currents in the classical ST-DTC strategy for dual-three phase PMSM drives,

while preserving its advantages, such as simple structure and good robustness. This paper is based on [12], much more clear description of the two-step process is proposed, and detailed experimental results have been shown to verify the proposed method. The remainder of this paper consists of the following sections. In section 2, machine modeling and analysis based on the vector space decomposition technique is described. In section 3, basic principle of switching-table-based DTC strategy for dual-three phase drives is exposed. Then a two-step process to select the most appropriate voltage vector is presented in section 4: firstly, according to the classical switching table and outputs of the hysteresis regulators, selecting the voltage vector group to meet the requirement of torque and flux control, secondly, choosing the most suitable voltage vector from that group, basing on the position of the harmonic stator flux, to reduce the harmonic currents. Experimental results are provided in section 5 to demonstrate the validity of the proposed solutions.

2 Machine model and analysis of inverter voltage vectors

2.1. Machine model

To develop the dual-three phase PMSM model, the following assumptions and approximations have been adopted:

1) Machine windings are sinusoidally distributed;

2) The magnetic saturation, the mutual leakage inductance, and the core losses are neglected.

According to the VSD approach [5], the original six-dimensional (6-D) system of the machine can be decomposed into three two-dimensional (2-D) uncoupled subsystems: $\alpha\beta$, z_1z_2, and o_1o_2. This transformation has the property to separate harmonics into three groups:

1) The fundamental components of the machine variables (could be voltage, current, flux) and the harmonics of order $k=12m\pm1, (m=1, 2, 3,...)$ are mapped to the $\alpha\beta$ subspace. These variables are related to the electromechanical energy conversion.

2) The harmonics with $k=6m\pm1, (m=1, 3, 5,...)$, i.e., the 5th, 7th,… harmonics are transformed into the z_1z_2 subspace. These components are not related to electromechanical energy conversion.

3) The zero-sequence with $k=3m, (m=1, 3, 5,...)$ are mapped to the o_1o_2 subspace to form the classical zero sequence components.

The final model can be expressed in stationary reference frame as:

$$\boldsymbol{V}_{s\alpha\beta} = R_s \boldsymbol{I}_{s\alpha\beta} + p\boldsymbol{\psi}_{s\alpha\beta} \tag{1}$$

$$\boldsymbol{\psi}_{s\alpha\beta} = L_s \boldsymbol{I}_{s\alpha\beta} + \boldsymbol{\psi}_{r\alpha\beta} \tag{2}$$

$$\boldsymbol{\psi}_{r\alpha\beta} = \psi_f e^{j\theta_r} \tag{3}$$

$$\boldsymbol{V}_{sz_1z_2} = R_s \boldsymbol{I}_{sz_1z_2} + p\boldsymbol{\psi}_{sz_1z_2} \tag{4}$$

$$\boldsymbol{\psi}_{sz_1z_2} = L_{ls} \boldsymbol{I}_{sz_1z_2} \tag{5}$$

$$\boldsymbol{V}_{so_1o_2} = R_s \boldsymbol{I}_{so_1o_2} + p\boldsymbol{\psi}_{so_1o_2} \tag{6}$$

$$\boldsymbol{\psi}_{so_1o_2} = L_{ls} \boldsymbol{I}_{so_1o_2} \tag{7}$$

$$T_e = 3P(\psi_{s\alpha} i_{s\beta} - \psi_{s\beta} i_{s\alpha}) \tag{8}$$

where, L_s=L_{ls}+3L_m is the stator inductance.

It should be mentioned that, if the two stator sets have isolated neutral points, as shown in Fig. 1, it can be deduced that all the vectors of o_1o_2 subspace are mapped to the origin, hence no currents flow in the o_1o_2 subspace according to (6) and (7). Therefore, the machine model can be reduced to two sets of decoupled equations corresponding to the machine $\alpha\beta$ and z_1z_2 subspaces. The detailed derivation can be found in [5].

Based on (8), after using VSD approach, torque and flux production involves only $\alpha\beta$ components, which makes the machine control as simple as the case of three phase machine. However, it also can be seen from (4) and (5) that the z_1z_2 components are responsible for the large circulating harmonic currents because of the small impedance in the z_1z_2 subspace. Therefore, the applied voltage vectors should contain not only the voltage commands in $\alpha\beta$ components but also the voltage commands to minimize the average amplitude of z_1z_2 components.

2.2. Analysis of the inverter voltage vectors

Owing to its six inverter legs, dual-three phase system contains 2^6=64 inverter voltage vectors, much more than three phase system. By neglecting the zero voltage vectors, the $\alpha\beta$ and z_1z_2 subspace voltage vectors can be shown in Figs. 2 (a) and (b), respectively. It should note that voltage vector number in Fig. 2 is termed based on binary value of V_i=$S_Z$$S_Y$$S_X$$S_C$$S_B$$S_A$ considering V_i as a 6-digit binary number, where value of each phase switching component S_i is set as "1" when its equivalent stator terminal is connected to DC link voltage rail and "0" if it is linked to zero voltage rail.

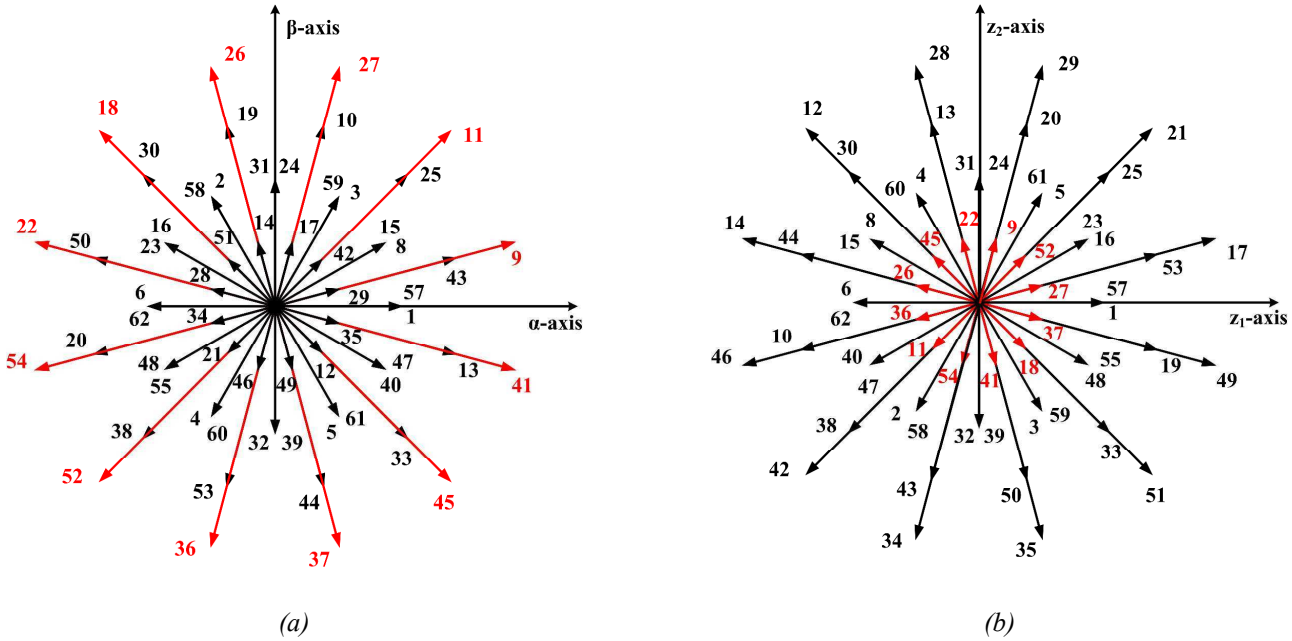

(a) *(b)*

Fig. 2. *Inverter voltage vectors in two subspaces:*

(a) αβ subspace

(b) z_1z_2 subspace

It can be seen from Fig. 2 that the outmost voltage vectors in the *αβ* subspace causing highest effect in the torque production are exactly the ones having the lowest influence in the z_1z_2 subspace - innermost voltage vectors in the z_1z_2 subspace. Therefore, the outermost voltage vectors in the *αβ* subspace are often chosen for controlling dual-three phase machine drive to maximize the efficiency of system and, at the same time, minimize losses because of the fact that voltage vector components in the z_1z_2 subspace do not contribute to rotating air gap flux but cause stator harmonic currents and result in losses.

3 Classical DTC scheme

As stated above, in term of torque control, the machine model of a dual-three phase PMSM is the same as the single three-phase PMSM. Therefore, the classical DTC strategy for the three phase system can be easily extrapolated to the dual-three phase PMSM systems, as shown in Fig. 3. It is obvious that, compared to the ST-DTC for three-phase drives, the only change is that the classical CLARK transformation (*abc*→*αβ0*) is replaced by a new transformation [T_6] (*abcxyz*→ $\alpha\beta z_1z_2o_1o_2$) as follows:

$$[T_6]=\frac{1}{3}\begin{bmatrix} 1 & \cos\frac{4\pi}{6} & \cos\frac{8\pi}{6} & \cos\frac{\pi}{6} & \cos\frac{5\pi}{6} & \cos\frac{9\pi}{6} \\ 0 & \sin\frac{4\pi}{6} & \sin\frac{8\pi}{6} & \sin\frac{\pi}{6} & \sin\frac{5\pi}{6} & \sin\frac{9\pi}{6} \\ 1 & \cos\frac{8\pi}{6} & \cos\frac{4\pi}{6} & \cos\frac{5\pi}{6} & \cos\frac{\pi}{6} & \cos\frac{9\pi}{6} \\ 0 & \sin\frac{8\pi}{6} & \sin\frac{4\pi}{6} & \sin\frac{5\pi}{6} & \sin\frac{\pi}{6} & \sin\frac{9\pi}{6} \\ 1 & 1 & 1 & 0 & 0 & 0 \\ 0 & 0 & 0 & 1 & 1 & 1 \end{bmatrix} \tag{9}$$

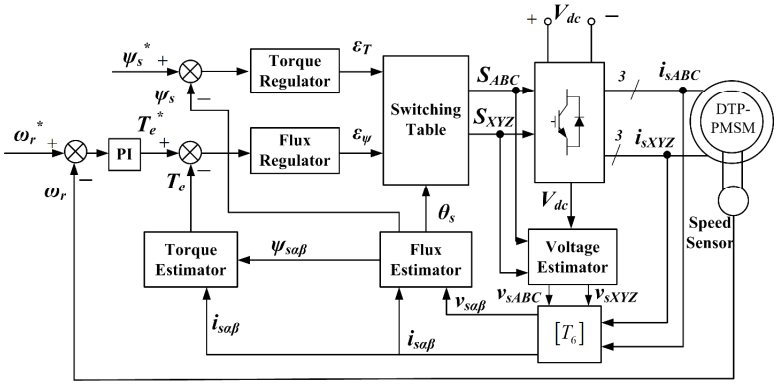

Fig. 3 *Classical ST-DTC diagram of dual-three phase PMSM drives*

Consequently, based on the estimated stator flux position, the $\alpha\beta$ subspace can be divided into 12 sectors, Fig. 4(a). Then, torque and flux regulators are used to generate the inverter vectors by using a switching table, as shown in Fig. 3. It should be noted that, in order to achieve the best torque dynamic performance, only voltage vectors from the outermost layer of a 12-sided polygon in the $\alpha\beta$ subspace together with the zero vectors will be selected to structure the switching table. Fundamentally, when the stator flux vector $\psi_{s\alpha\beta}$ lies in sector k, as shown in Fig. 4(b), instantaneous control of stator flux and torque can be achieved via employing appropriate voltage vectors according to Table 1, where all the voltage vectors are selected to maximize torque response.

Table 1 Classical switching table for DTC-based dual-three phase drive

SECTOR K	E_T =1	E_T =-1	E_T =0
ε_ψ =1	V_{k+2}	V_{k-3}	V_{zero}
ε_ψ =-1	V_{k+3}	V_{k-4}	V_{zero}

In Table 1, the torque and stator flux control signals ε_T and ε_ψ are generated by torque and flux regulators, respectively, which are defined as

$$\varepsilon_T = \begin{cases} 1, \text{ to increase } T_e \\ 0, \text{ to keep } T_e \\ -1, \text{ to decrease } T_e \end{cases} ; \varepsilon_\psi = \begin{cases} 1, \text{ to increase } \psi_s \\ -1, \text{ to decrease } \psi_s \end{cases} \quad (10)$$

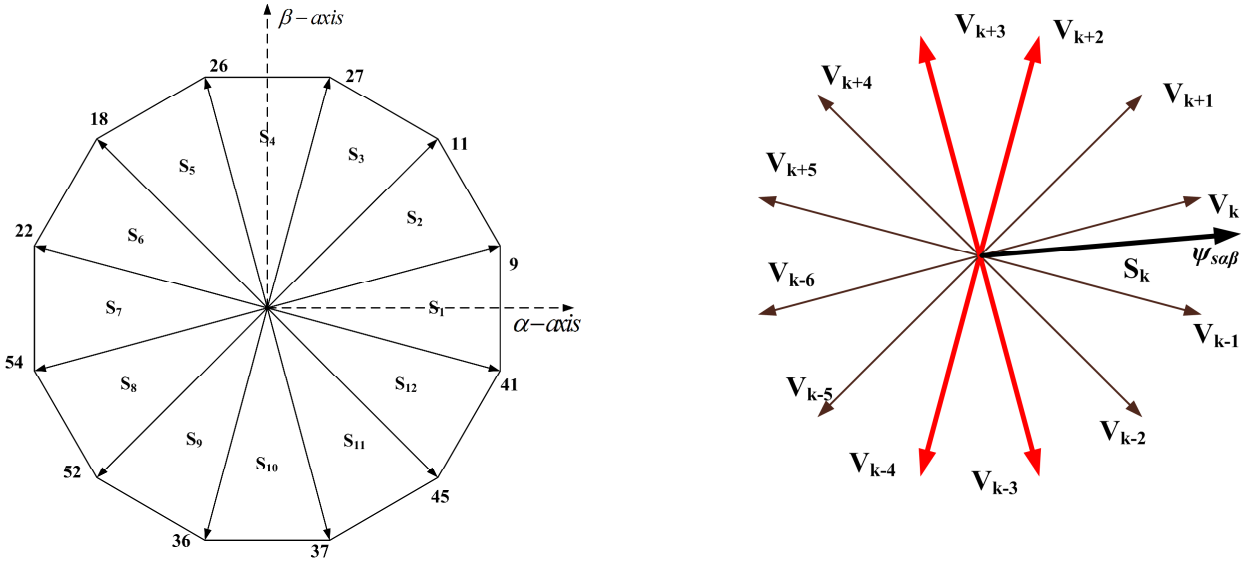

(a) *(b)*

Fig. 4. *Basic principle of classical ST-DTC scheme:*

(a) Definition of 12 sectors in αβ subspace

(b) Selection of voltage vectors when the stator flux lies in sector k

The classical ST-DTC strategy is very easy to implement. However, since only the $\alpha\beta$ components associated with torque production are regulated under this control method, although the vectors of outmost layer in the $\alpha\beta$ subspace has the lowest amplitude in the z_1z_2 subspace, the z_1z_2 components are still freely circulated inside the machine. Large harmonic currents will thereby be observed because of the only limitation is the leakage inductance, as shown in (5).

Therefore, it is obvious that a DTC technique taking into account the z_1z_2 components to minimize their effects on the harmonic currents is essentially required.

4 Proposed DTC scheme

It can be seen from (5) that in the z_1z_2 subspace, the unexpected harmonic current is proportional to the stator flux in the z_1z_2 subspace ψ_{sz1z2}. Therefore, minimizing the stator flux ψ_{sz1z2} is an effective way to reduce the harmonic currents i_{sz1z2}.

It is obvious that, in the $\alpha\beta$ subspace, there are three voltage vectors pointing to the same direction, e.g. V_9, V_{43} and V_{29} in Fig. 5(a), having nearly similar effects on torque and flux control except that the larger vectors provide faster responses. However, in the z_1z_2 subspace shown in Fig. 5(b), V_9 and V_{29} still point to the same direction, while V_{43} points to the oppositional direction

compared to V_9 and V_{29}, and therefore cause oppositional effects on the variation of z_1z_2 flux ψ_{sz1z2}.

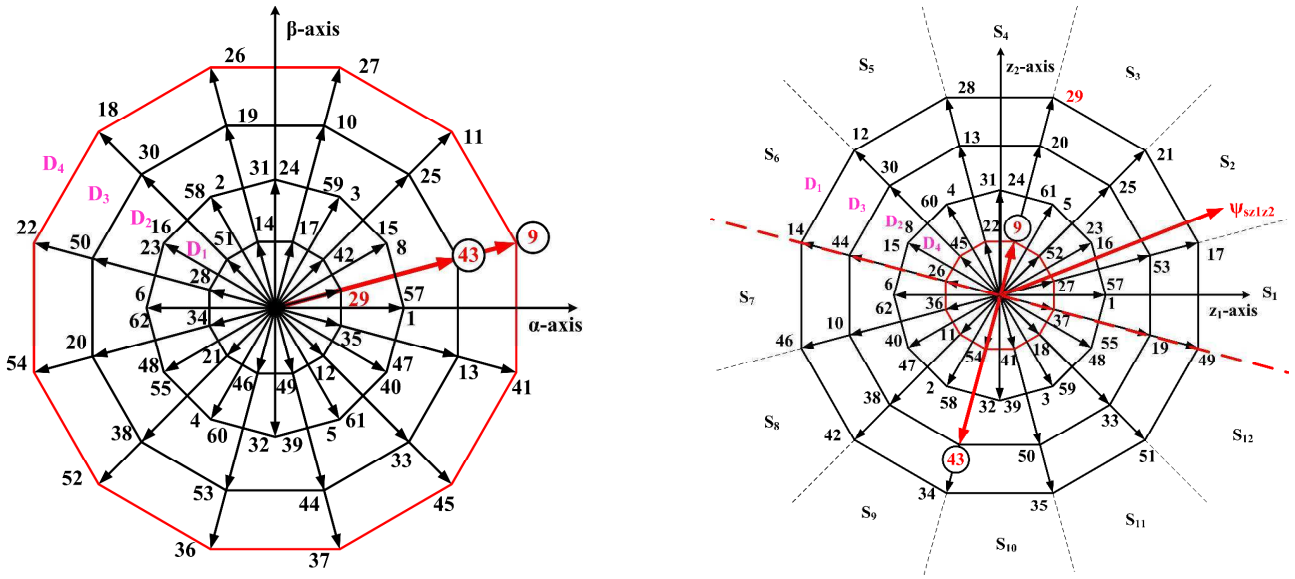

(a) *(b)*

Fig. 5. *Proposed voltage vector selection strategy in two subspaces:*

(a) αβ subspace

(b) z_1z_2 subspace

In order to describe more clearly, the active vectors in the $\alpha\beta$ subspace are classified into 4 layers according to their amplitudes, from innermost to outermost: D_1, D_2, D_3, D_4, whereas in the z_1z_2 subspace the sequence, from innermost to outermost: D_4, D_2, D_3, D_1, as shown in Fig. 5. Therefore, it can be easily deduced that the vectors of D_1 and D_4 have the same effect on ψ_{sz1z2}, while vectors in D_3 layer have the oppositional effect. Consequently, by introducing the vectors of D_3 layer into control, the amplitude of ψ_{sz1z2} is possible to be reduced, and then the corresponding harmonic currents will be decreased. Owing to the same direction both in $\alpha\beta$ subspace and z_1z_2 subspace, but much smaller amplitude in the $\alpha\beta$ subspace and larger amplitude in the z_1z_2 subspace compared to D_4, the vectors of D_1 will not be considered. The vectors of D_2 will not be employed either due to the different direction both in the $\alpha\beta$ and z_1z_2 subspace compared to D_1, D_3 and D_4.

Thus, by dividing the z_1z_2 subspace into two half-circle subspaces of which diameter is orthogonal to V_9 and V_{43}, Fig. 5(b), it is obvious that if the z_1z_2 flux vector is located in one half-circle subspace, voltage vector in the other half-circle subspace should be adopted to minimize the z_1z_2 stator flux magnitude and then reduce z_1z_2 current harmonic components. For example, if ψ_{sz1z2} locates in sector2 in z_1z_2 subspace, as shown in Fig. 5(b), then applying V_9 will led to the increasing of amplitude of ψ_{sz1z2}, while applying V_{43} will result in the decreasing of amplitude of ψ_{sz1z2}. This is exactly the key reason why there is large harmonic

currents in the classical ST-DTC controlled dual-three phase machines, although the vectors of outmost layer in the $\alpha\beta$ subspace has the lowest amplitude in the z_1z_2 subspace. Hence, V_{43}, instead of V_9, should be employed as that in the classical ST-DTC strategy. Similar results can be extended to other sectors. It should be pointed out that, as shown in Fig. 5(b) and Fig. 4(a), the definition of the sectors of z_1z_2 subspace is the same as that of $\alpha\beta$ subspace, i.e.,

Sector k:

$$-\frac{\pi}{12}+\frac{\pi}{6}(k-1) \le \theta_{s\alpha\beta}, \theta_{sz1z2} < \frac{\pi}{12}+\frac{\pi}{6}(k-1),\ k=1,2,...12 \tag{11}$$

Consequently, based on the principle above, there are two steps to pick an appropriate voltage vector.

1) According to the sector of $\psi_{s\alpha\beta}$ in the $\alpha\beta$ subspace and the outputs of hysteresis comparators, one vector in D_3 and one vector in D_4, which have the same direction in the $\alpha\beta$ subspace and are defined as one group in this paper, are chose as candidates;

2) Based on the position of ψ_{sz1z2} in the z_1z_2 subspace, the vector which can reduce the amplitude of ψ_{sz1z2} will be chosen from the selected group.

It is obvious that the first step is the same to the collection of vectors in the classical ST-DTC, therefore, the vector groups can be chosen from Table 1, and the vector group is also named with the vector chosen from Table 1. Consequently, a switching table for the second step is presented in Table 2. For example, if the vector group 9 is selected from Table 1 in the first step, only when ψ_{sz1z2} lies in sectors 1-6, V_9 will be employed as that in the classical ST-DTC strategy, otherwise, V_{43} will be adopted to decrease the amplitude of ψ_{sz1z2}.

Table 2 Switching table for step two in the proposed DTC of dual-three phase drive

VECTOR GROUP G_1	SECTOR OF Ψ_{SZ1Z2}	SELECTED VECTOR	VECTOR GROUP G_1	SECTOR OF Ψ_{SZ1Z2}	SELECTED VECTOR
9	7,8,9,10,11,12	V_9	54	1,2,3,4,5,6	V_{54}
	1,2,3,4,5,6	V_{43}		7,8,9,10,11,12	V_{20}
11	12,1,2,3,4,5	V_{11}	52	6,7,8,9,10,11	V_{52}
	6,7,8,9,10,11	V_{25}		12,1,2,3,4,5	V_{38}
27	5,6,7,8,9,10	V_{27}	36	11,12,1,2,3,4	V_{36}
	11,12,1,2,3,4	V_{10}		5,6,7,8,9,10	V_{53}
26	10,11,12,1,2,3	V_{26}	37	4,5,6,7,8,9	V_{37}
	4,5,6,7,8,9	V_{19}		10,11,12,1,2,3	V_{44}
18	3,4,5,6,7,8	V_{18}	45	9,10,11,12,1,2	V_{45}
	9,10,11,12,1,2	V_{30}		3,4,5,6,7,8	V_{33}
22	8,9,10,11,12,1	V_{22}	41	2,3,4,5,6,7	V_{41}
	2,3,4,5,6,7	V_{50}		8,9,10,11,12,1	V_{13}

The block diagram of the proposed ST-DTC strategy is illustrated in Fig. 6. Compared to the block diagram of classical ST-DTC strategy as shown in Fig. 3, only one harmonic suppression module consisting of the flux estimator in the z_1z_2 subspace and switching table 2 is added to decrease the stator harmonic currents, therefore, the merits of the classical DTC strategy, i.e. simple structure and good robustness, are still preserved.

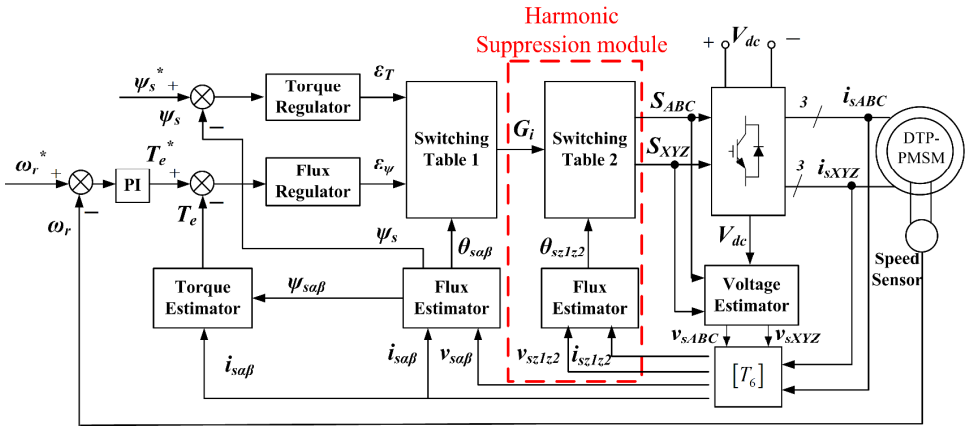

Fig. 6 *Block diagram of proposed ST-DTC strategy*

In general, the proposed ST-DTC strategy is simple as only the position information of the stator flux vector ψ_{sz1z2} is required, as shown in Fig. 6. As same as the situation in the $\alpha\beta$ reference frame, the problem of flux drifting still exists in the z_1z_2 reference frame, which will not only fail to reduce the harmonic currents, but also lead to the decrease of the average torque. Therefore, a low pass filter is employed to replace the pure integrator. On the other hand, slight reduction of the utilization rate of DC supply will inevitably occur because of the difference in magnitudes between voltage vectors in D_3 and D_4. To be more specific, the amplitudes of the vectors in D_3 and D_4 can be calculated according to Fig. 2 (a), taking V_9 and V_{43} as example, as follows:

$$D_4:\ |V_9| = 2A\cos 15^0 = \frac{\sqrt{6}+\sqrt{2}}{2}A \tag{12}$$

$$D_3:\ |V_{43}| = 2A\cos 45^0 = \sqrt{2}A \tag{13}$$

where A is the amplitude of the synthesize vector of one set of three-phase drive.

It can be seen from Table 2 that, for each vector group selected from Table 1, the chance to select the vector from D_3 or D_4 can be considered the same. Therefore, the utilization rate of DC supply of proposed ST-DTC strategy compared to that of classical ST-DTC strategy can be estimated as

$$\eta = \frac{|V_9|*T_s/2 + |V_{43}|*T_s/2}{|V_9|*T_s}*100\% = \frac{\frac{\sqrt{6}+\sqrt{2}}{2}A + \sqrt{2}A}{2*\frac{\sqrt{6}+\sqrt{2}}{2}A}*100\% = 86.60\% \tag{14}$$

In summary, this proposed ST-DTC strategy only slightly changes average amplitude of the applied voltage vector. Therefore, for the torque performance, simple structure and good dynamic performance have been preserved, which results in the similar good robustness to the external disturbances, which will be verified by the experimental results.

For the sake of completeness, two issues which are usually considered as important in implementing ST-DTC strategies should be mentioned here:

Remark1: It is true that the hysteresis band has an important effect on the steady-state performance of torque. Since this paper focuses on the reduction of harmonic currents and the hysteresis band has limited effect on the harmonic current, we do not expand this analysis here. The detailed analysis of hysteresis band can be referred to literature [13]. However, we have reduced the steady-state error of torque by using a band-shifted method which has been successfully applied on the ST-DTC for three phase drives [14].

Remark2: For the real-time system, there are many factors that will cause the harmonic currents, such as the harmonic supply voltage, dead-time, and inverter nonlinearity, etc. However, for the ST-DTC, the harmonic supply voltage is the most important reason to the large harmonic currents, according to VSD approach. By employing this modified ST-DTC strategy, the majority

of the harmonic currents have been suppressed, and at the same time, the merits of the classical direct torque control, i.e. simple structure and good dynamic performance, are still preserved. Therefore, for the sake of simplicity and parameter independence, other factors are not compensated in this paper.

5 Experimental Results

The experimental setup consists of a DC power supply, a dual-three phase inverter, a dSPACE DS1005 digital controller, and a laboratory prototype of the dual-three phase PMSM. The parameters of test machine are listed in Table 3. The overall control schemes with classical and proposed DTC strategies are shown in Figs. 3 and 6, respectively. The sample frequency is 10 kHz, and the DC-Bus voltage is set to 40V. All the results were captured using dSPACE software, and then plotted using Matlab.

Table 3 Parameters of test machine

NUMBER OF POLE PAIRS	5
Permanent magnet flux	73.4mWb
Stator resistance	1.096Ω
d-axis and *q*-axis inductances	2.142mH
Rated speed	400rpm

5.1 Steady-state performance of different ST-DTC strategies

Figs. 7-9 show the experimental results of the classical and proposed ST-DTC strategies for dual-three phase PMSM drives. The rotor speed reference and stator flux reference are set to 300rpm, 0.075Wb, respectively, while the load is about 2.5Nm (partially loaded). It can be seen from Fig. 7 that the torque, stator flux can be controlled well both in the classical and proposed DTC strategies. The torque ripple is slightly reduced due to the decrease of the average amplitude of the applied voltage in one sampling period. The steady-state error of torque has been significantly reduced by using the band-shifted torque regulator [14]. However, it is obvious that the phase currents of the classical DTC strategy are seriously non-sinusoidal, Fig. 8 (a). This is because the components in the z_1z_2 subspace are not controlled in the classical ST-DTC strategy, hence, the stator flux in the z_1z_2 subspace ψ_{sz1z2} is not negligible any more, as shown in Fig. 8 (d), resulting in the large harmonic currents, Fig. 8 (b), (c). By using the proposed two-step process to choose the appropriate voltage vector, the stator flux in the z_1z_2 subspace ψ_{sz1z2} is negligible compared to that in the $\alpha\beta$ subspace $\psi_{s\alpha\beta}$, Fig. 9 (d). Therefore, the harmonic currents are significantly reduced, and consequently much more sinusoidal phase currents are achieved, Fig. 9 (a), (b), (c).

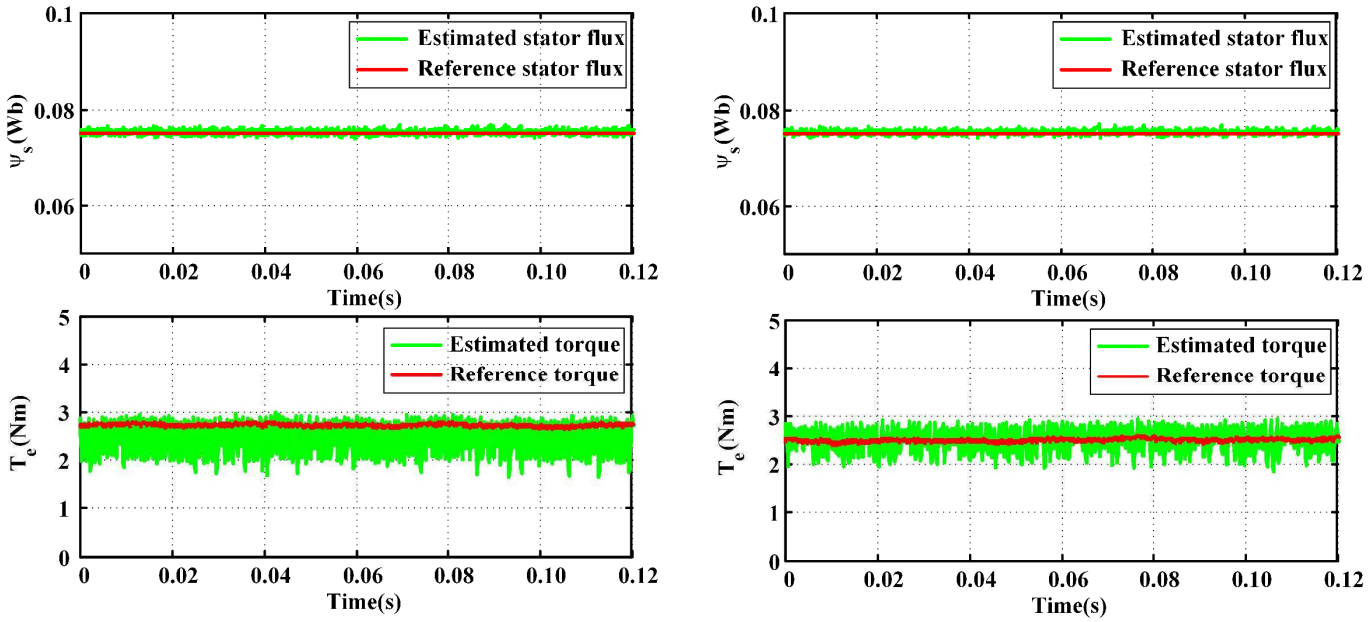

Fig. 7. *Steady-state performance of torque and stator flux using different DTC strategies.*

(a) Classical ST-DTC strategy

(b) Proposed ST-DTC strategy

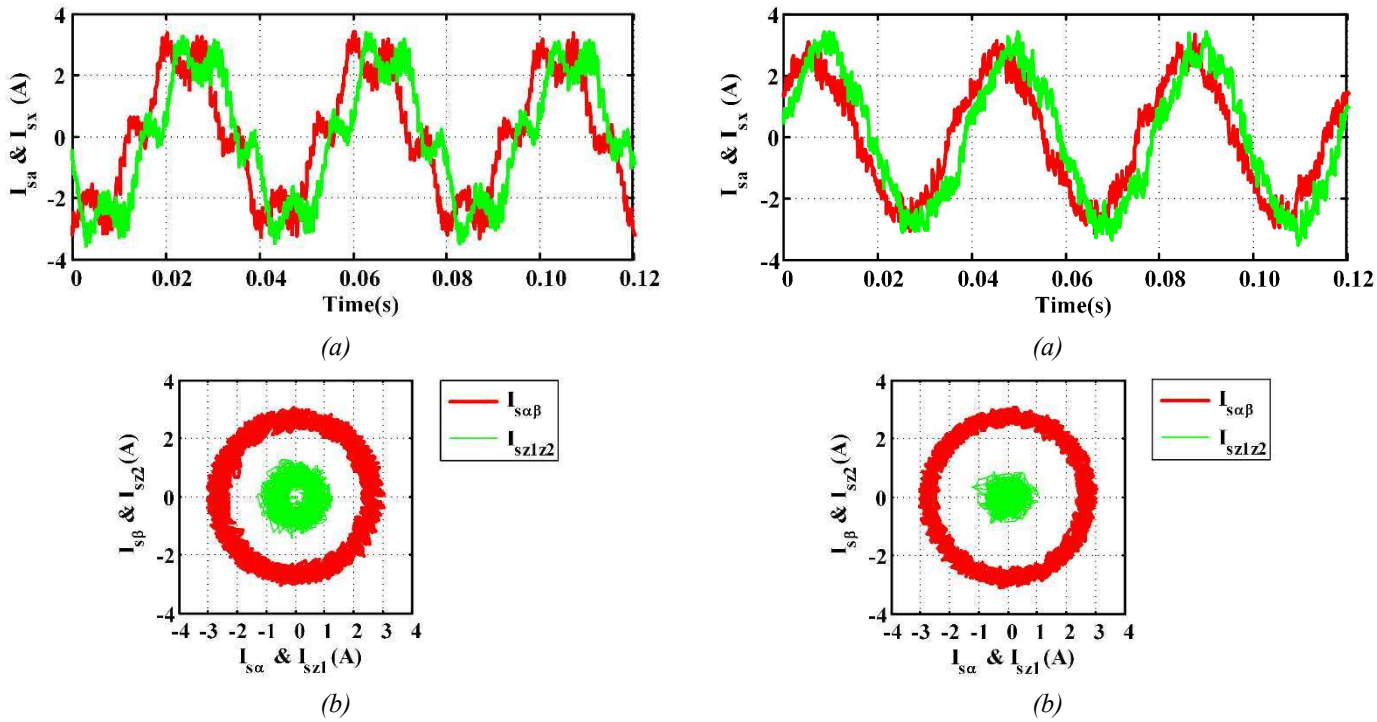

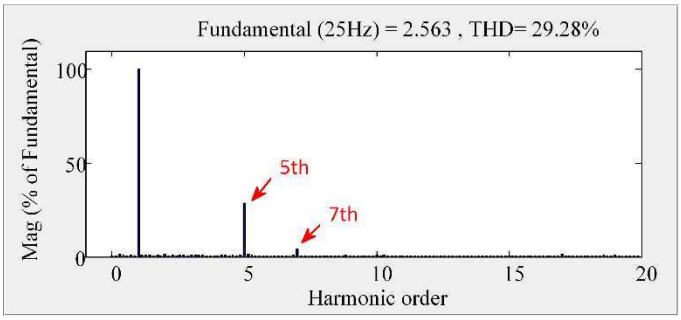

(c)

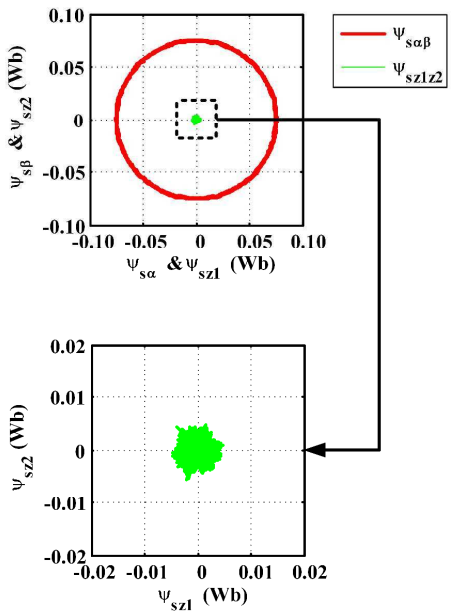

(d)

Fig. 8. *Steady-state performance of classical ST-DTC strategy*

(a) Phase currents

(b) αβ and z_1z_2 current circles

(c) Phase current harmonic spectrum

(d) Stator flux circle

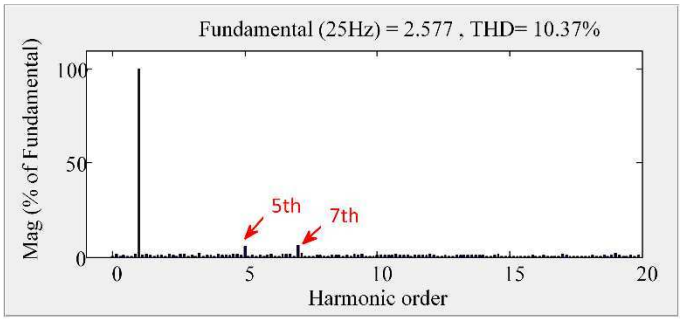

(c)

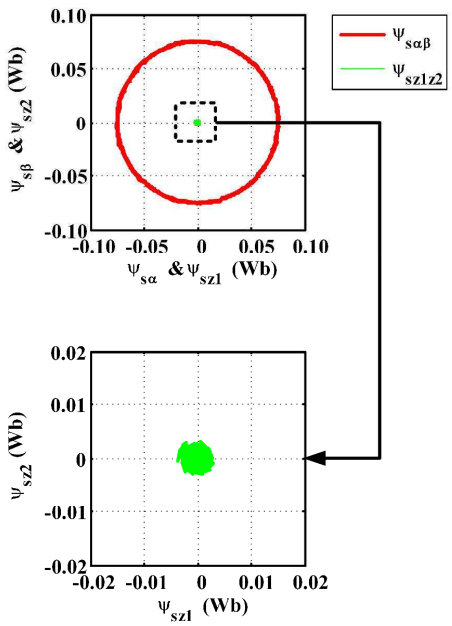

(d)

Fig. 9. *Steady-state performance of proposed ST-DTC strategy*

(a) Phase currents

(b) αβ and z_1z_2 current circles

(c) Phase current harmonic spectrum

(d) Stator flux circle

Since the harmonic components do not contribute the electromechanical energy conversion, both the stator flux ripple in the *αβ* subspace and the torque ripple are almost equal to those using classical ST-DTC strategy. Detailed quantitative results are given in Table 4, where the torque and stator flux ripples are calculated as

$$\psi_{s\_ripple} = \sqrt{\frac{1}{n}\sum_{i=1}^{n}(\psi_{s\_i} - \psi_{s\_av})^2} \tag{15}$$

$$T_{e\_ripple} = \sqrt{\frac{1}{n}\sum_{i=1}^{n}(T_{e\_i} - T_{e\_av})^2} \tag{16}$$

where T_{e_i} and ψ_{s_i} are the instant value of torque and stator flux, respectively, whist T_{e_av} and ψ_{s_av} are the average values of

torque and stator flux, respectively.

In the switching-table-based DTC strategies, the switching frequency changes with the operating conditions. Therefore, the average commutation frequency f_{av}, which is calculated by counting the total commutation instants of one phase leg over a fixed period, is used to indicate the switching losses [15].

Table 4 Experimental results of classical and proposed ST-DTC strategies

	CLASSICAL ST-DTC	PROPOSED ST-DTC
Ripple of stator flux, ψ_{s_ripple} *(Wb)*	5.4279e-004	4.9134e-004
Ripple of torque, T_{e_ripple} *(Nm)*	0.3106	0.2392
THD of phase-a current, i_{a_THD} *(%)*	29.28	**10.37**
Average commutation frequency, f_{av} *(kHz)*	2.7572	3.5472

It can be seen from Table 4, because of the decreasing of the average amplitude of applied voltage vectors, both the stator flux and torque ripples of the proposed ST-DTC strategy slightly decreases compared to the classical ST-DTC strategy. The THD of phase current has been decreased by 64.58%, from 29.28% to 10.37%, due to the significant reduction of harmonic currents in z_1z_2 subspace, Fig. 9 (b). One drawback of the proposed method is that the average commutation frequency will increase a little, 0.79 kHz in this case, which results in a little increase of the losses. This is reasonable because in the proposed strategy two switching tables are needed to choose the most appropriate voltage vector, which makes the voltage vectors change more frequently compared to the classical one. Of course, it is acceptable to achieve a significant reduction of harmonic currents at the low price of increasing the average commutation frequency.

Table 5 shows the THD of phase-a current for classical and proposed ST-DTC strategies under the condition of same rotor speed which is 400 rpm (rated speed) and various load torque from 1Nm to 3Nm (rated load). It can be seen from table 5 that the proposed ST-DTC strategy can significantly reduce the THD of phase currents under a wide range of load conditions.

Table 5 THD of phase-a current for classical and proposed ST-DTC strategies

400rpm	CLASSICAL ST-DTC	PROPOSED ST-DTC
1Nm	52.14%	26.22%
2Nm	33.84%	14.65%
3Nm (rated load)	26.06%	9.83%

5.2 Dynamic performance of inner torque loop control for conventional and proposed DTC

As mentioned above, the utilization rate of DC supply is slightly reduced in the proposed DTC strategy. Therefore, it is necessary to check whether the dynamic performance of torque control will deteriorate accordingly.

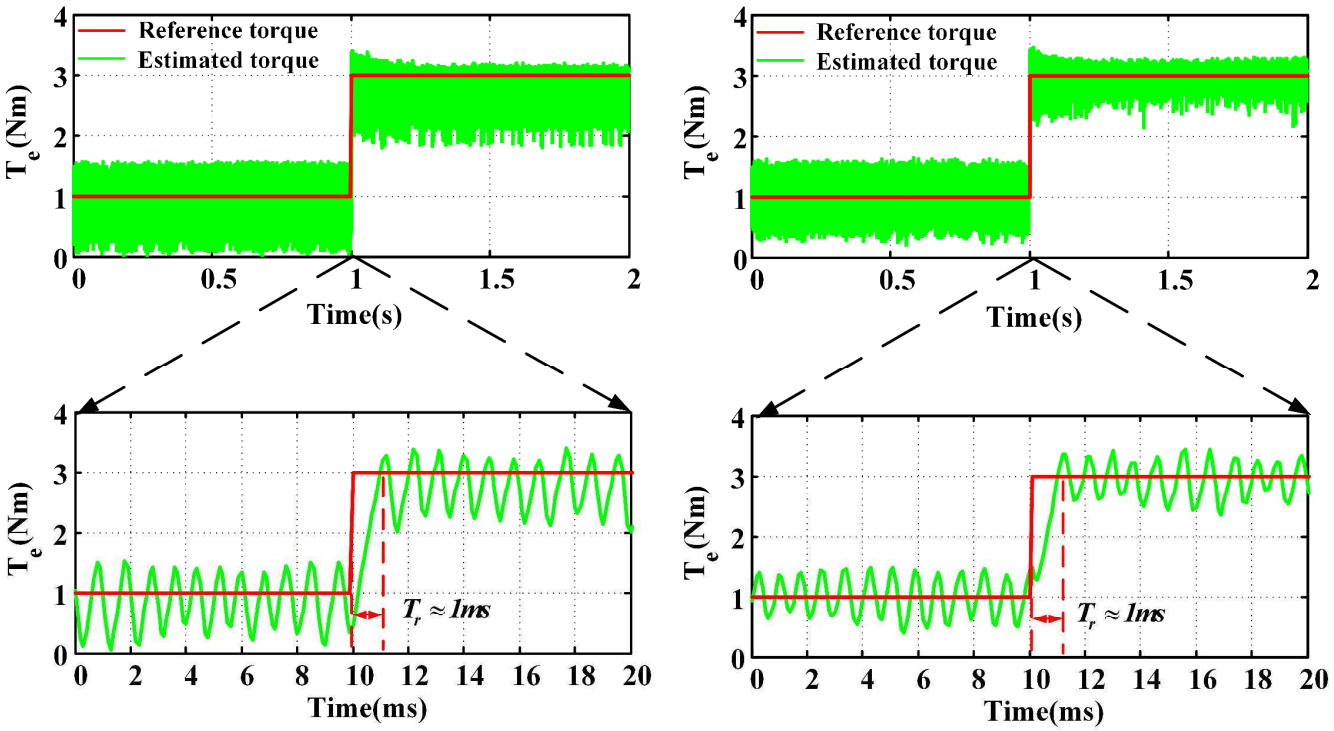

Fig. 10. *Dynamic performance of inner torque loop control using different DTC methods: reference torque:1Nm to 3Nm*

(a) Classical ST-DTC strategy

(b) Proposed ST-DTC strategy

Fig. 10 shows the dynamic response of torque when the torque reference changes from 1Nm to 3Nm, with the speed open-loop control, i.e. with inner torque control only, for both conventional and improved DTC strategies. It is clear that the torque can reach the reference torque in less than 1ms, similar to that of the conventional DTC strategy. Hence, the proposed strategy will not deteriorate the dynamic torque performance.

5.3 Dynamic responses to external load disturbance for proposed DTC strategy

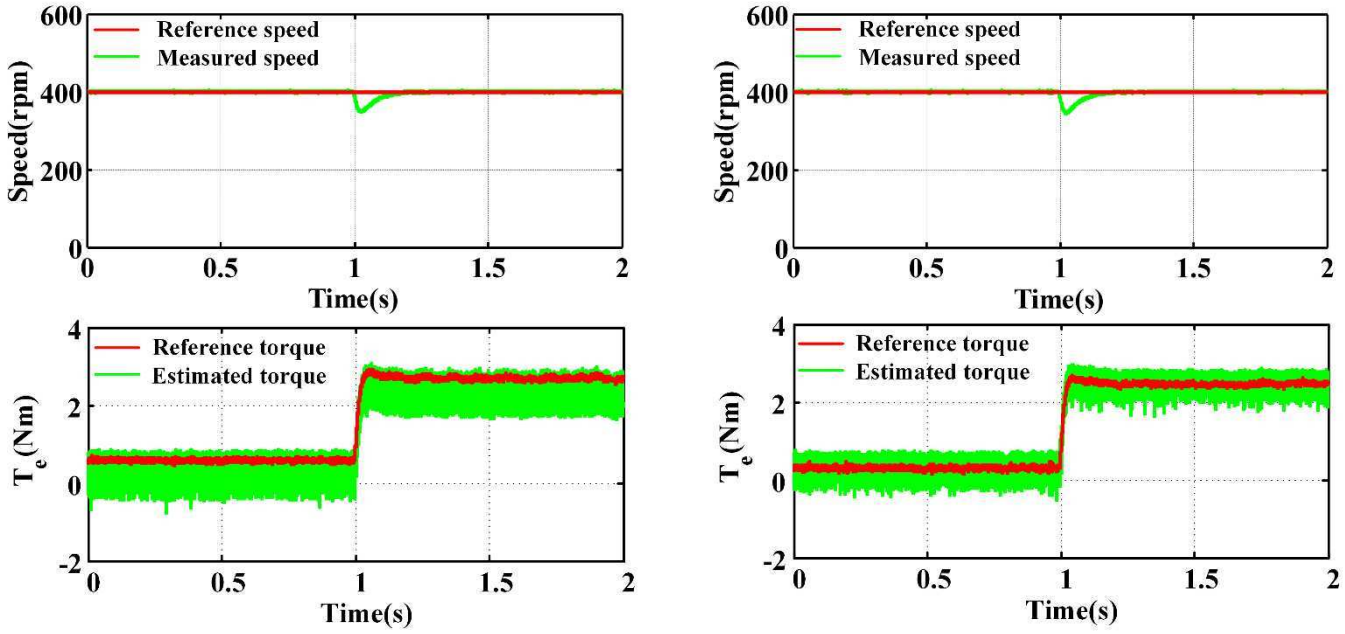

Fig. 11. *Responses to external disturbance of different DTC strategies.*

(a) Classical ST-DTC strategy

(b) Proposed ST-DTC strategy

The responses to external load disturbance are compared between the conventional DTC and the proposed method. When the motor is operated under steady-state of 400rpm without load, the external load about 2.5Nm is suddenly added at the instant of 1.0s, Fig. 11. It can be seen that the torque generated with the proposed method can follow the reference produced by the speed regulator as good as the conventional one. The speeds in both the conventional and the proposed strategy can back to its original value in less than 0.3s.

Therefore, the experimental results prove that the proposed DTC method can preserve the good robustness against external load disturbance as in the conventional DTC.

6 Conclusion

This paper presents application of ST-DTC to dual-three phase PMSM drives using the vector space decomposition technique. To minimize the unexpected large stator harmonic currents, a two-step process voltage vector selection scheme has been proposed. Classical ST-DTC strategy only controls the variables in the $\alpha\beta$ subspace relating to the torque production, so the uncontrolled flux space vector in the other subspace results in substantial stator harmonics currents. The proposed DTC strategy not only controls the variables in the $\alpha\beta$ subspace, but also significantly reduces the magnitude of the flux space vector in the z_1z_2 subspace, which results in considerably lower harmonics in stator currents. The experimental results verify that the proposed

methods can significantly reduce the stator current harmonics. Furthermore, since only one harmonic suppression module consisting of the flux estimator in the z_1z_2 subspace and a switching table is added, the merits of the classical direct torque control, i.e. simple structure and good robustness, are still preserved.

7 References

[1] Bojoi, R., Lazzari, M., Profumo, F., and Tenconi, A.: 'Digital field-oriented control for dual three-phase induction motor drives,' *IEEE Trans.Ind. Appl.*, 2003, **39**, (3), pp. 752-760.
[2] Bojoi, R., Farina, F., Griva, G., Profumo, F., and Tenconi, A.: 'Direct torque control for dual three-phase induction motor drives,' *IEEE Trans.Ind. Appl.*, 2005, **41**, (6), pp. 1627-1636.
[3] Levi, E.: 'Multiphase electric machines for variable-speed applications,' *IEEE Trans.Ind. Electron.*, 2008, **55**, (5), pp. 1893-1909.
[4] Gopakumar, K., Sathiakumar, S., Biswas, S. K., and Vithayathil J.: 'Modified current source inverter fed induction-motor drive with reduced torque pulsations,' *Iee Proceedings-B Electr. Power Appl.*, 1984, **131**, pp. 159-164.
[5] Zhao, Y. and Lipo, T. A.: 'Space vector pwm control of dual three-phase induction machine using vector space decomposition,' *IEEE Trans.Ind. Appl.,* 1995, **31**, (5), pp. 1100-1109.
[6] Abbas, M. A., Christen, R., and Jahns, T. M.: 'Six-phase voltage source inverter driven induction motor,' *IEEE Trans.Ind. Appl.*, 1984, **20**, (5), pp. 1251-1259.
[7] Hadiouche, D., Baghli, L., and Rezzoug, A.: 'Space-vector pwm techniques for dual three-phase ac machine: Analysis, performance evaluation, and dsp implementation,' *IEEE Trans.Ind. Appl.*, 2006, **42**, (4), pp. 1112-1122.
[8] Hatua, K. and Ranganathan, V. T.: 'Direct torque control schemes for split-phase induction machine,' *IEEE Trans.Ind. Appl.*, 2005, **41**, (5), pp. 1243-1254.
[9] Gao, Y. and Parsa, L.: 'Modified direct torque control of five-phase permanent magnet synchronous motor drives,' *Applied Power Electronics Conference, APEC 2007 - Twenty Second Annual IEEE*, 2007, pp. 1428-1433.
[10] Zheng, L. B., Fletcher, J. E., Williams, B. W., and He, X. N.: 'A novel direct torque control scheme for a sensorless five-phase induction motor drive,' *IEEE Trans. Ind. Electron.*, 2011, **58**, (2), pp. 503-513.
[11] Gao, L. L., Fletcher, J. E., and Zheng, L. B.,: 'Low-speed control improvements for a two-level five-phase inverter-fed induction machine using classic direct torque control,' *IEEE Trans. Ind. Electron.*, 2011, **58**, (7), pp. 2744-2754.
[12] Hoang, K. D., Zhu, Z. Q., and Foster, M.: 'Optimum look-up table for reduction of current harmonics in direct torque controlled dual three-phase permanent magnet brushless ac machine drives,' *6th IET International Conference on Power Electronics, Machines and Drives,*, 2012, pp. 1-6.
[13] Mathapati, S. and Bocker, J.: 'Analytical and offline approach to select optimal hysteresis bands of dtc for pmsm,' *IEEE Trans. Ind. Electron.*, 2013, **60**, (3), pp. 885-895.
[14] Zhu, Z. Q., Ren, Y., and Liu, J. M.: 'Improved torque regulator to reduce steady-state error of torque response for direct torque control of permanent magnet synchronous machine drives,' *IET, Electr. Power Appl.,* 2014, **8**, (3), pp. 108-116.
[15] Zhang, Y. and Zhu, J.: 'Direct torque control of permanent magnet synchronous motor with reduced torque ripple and commutation frequency,' *IEEE Trans. Power Electron.*, 2011, **26**, (1), pp. 235-248.